

# 330 mJ single-frequency Ho:YLF slab amplifier

H. J. Strauss,<sup>1,\*</sup> D. Preussler,<sup>1</sup> M. J. D. Esser,<sup>1</sup> W. Koen,<sup>1</sup> C. Jacobs,<sup>1</sup> O. J. P. Collett,<sup>1</sup> and C. Bollig<sup>1,2</sup>

<sup>1</sup>National Laser Centre, Council for Scientific and Industrial Research, P.O. Box 395, Pretoria 0001, South Africa

<sup>2</sup>Carl von Ossietzky Universität Oldenburg, Institut für Physik, AG Meeresphysik, Oldenburg D-26111, Germany

\*Corresponding author: hstrauss@csir.co.za

Received December 19, 2012; revised February 8, 2013; accepted February 16, 2013;  
posted February 20, 2013 (Doc. ID 182054); published March 20, 2013

We report on a double-pass Ho:YLF slab amplifier which delivered 350 ns long single-frequency pulses of up to 330 mJ at 2064 nm, with a maximum  $M^2$  of 1.5 at 50 Hz. It was end pumped with a diode-pumped Tm:YLF slab laser and seeded with up to 50 mJ of single-frequency pulses. © 2013 Optical Society of America

OCIS codes: 140.0140, 140.3070, 140.3280, 140.3570, 140.3580, 140.5680.

High-energy 2  $\mu\text{m}$  sources are sought after in a wide variety of applications, some of which are in defense, medicine, material processing, and remote sensing [1]. Ho doped into  $\text{YLiF}_4$  (YLF) is an excellent gain medium with which to obtain high-energy Q-switched 2  $\mu\text{m}$  pulses. This is because it has a high gain cross section, long upper level lifetime, and weak thermal lensing and is naturally birefringent [2,3]. Recently, diffraction-limited 2  $\mu\text{m}$  pulses with energies up to  $\sim 170$  mJ at 100 Hz have been demonstrated from a Ho:YLF master oscillator power amplifier [4] which was pumped with three 120 W Tm-fiber lasers. High average power 1.9  $\mu\text{m}$  Tm slab lasers can also be used as pump sources, especially for amplifiers where the good beam quality of fiber lasers is not required for the pump beam.

We recently demonstrated 210 mJ of single-frequency 2  $\mu\text{m}$  pulses using a Tm slab pumped, two crystal Ho:YLF and Ho:LuLF slab amplifier [5]. Subsequent simulations [6] indicated that using longer gain crystals and double passing the amplified beam would lead to a significant increase in gain.

Consequently we used two 0.5% doped, Ho:YLF slabs from VLOC in series. Both had dimensions 10 mm  $\times$  2 mm  $\times$  50 mm ( $c \times a \times a$ ) and were  $a$ -cut with their  $c$ -axis horizontal. The slabs were mounted with indium foil between custom-made, 22°C, water-cooled mounts. The experimental setup is illustrated in Fig. 1. The slabs were placed in series to provide a 200 mm gain length when double passed. As pump source, we used a Tm:YLF slab oscillator [5] delivering 187 W of output power. It was forced to operate on the pi-polarization by inserting a Brewster plate. Its wavelength was 1890 nm, which matched one of the strong absorption peaks of Ho:YLF. The beam had an  $M_x^2$  of 603 and an  $M_y^2$  of 2.78. The polarization was kept horizontal so that it was absorbed by the stronger absorbing pi-polarization of Ho:YLF. Its output power was monitored by a Gentec power meter (PS-310WB) placed behind a 99% mirror ( $M_2$ ). The pump beam was then steered into the Ho:YLF amplifier crystals using a high reflector (HR) at 1.9  $\mu\text{m}$ . To shape the beam, it was first collimated with an  $f = 100$  mm spherical lens ( $L_1$ ) and focussed into the Ho:YLF slabs with an  $f = 60$  mm spherical lens ( $L_3$ ). An  $f = 250$  mm horizontal cylindrical lens ( $L_2$ ) was used to match the horizontal focus position after  $L_3$  to that of the vertical. The Ho:YLF crystals were placed so that the pump focus was positioned in the gap between them,

accounting for the refractive index of YLF. The 1890 nm pump beam radii were measured with a pyroelectric camera (PY-III-CA from Spiricon) as 3.5 mm  $\times$  0.4 mm on the inner facing surfaces of the slabs and 4.5 mm  $\times$  0.45 mm ( $w_x \times w_y$ ) on the outer surfaces using the second moment method and had the focus intensity profile shown in Fig. 1. The transmitted pump power was measured with a power meter (LM 1000 HTD from Coherent) and the amplifier and pump laser were both enclosed in a dry air box to avoid spiking in the Tm:YLF laser output caused by water absorption.

The seed laser for the amplifier was a single-frequency, ring laser/amplifier system, pumped with a commercial 80 W 1940 nm Tm: fiber laser [7,8]. It delivered diffraction-limited output with energies of up to 70 mJ per pulse at 50 Hz, and had a pulse duration of 370 ns. The seed laser beam power was monitored by power meter  $\text{Pm}_2$  (LM 10 HTD from Coherent) placed behind a 95% partial reflector ( $M_4$ ). The seed beam was then steered into the Ho:YLF amplifier crystals using various HRs at 2  $\mu\text{m}$ . In the vertical direction, two cylindrical lenses  $L_4$ , ( $f_y = 774$  mm) and  $L_5$ , ( $f_y = 504$  mm) were used to focus the seed beam through the Ho:YLF crystals onto a

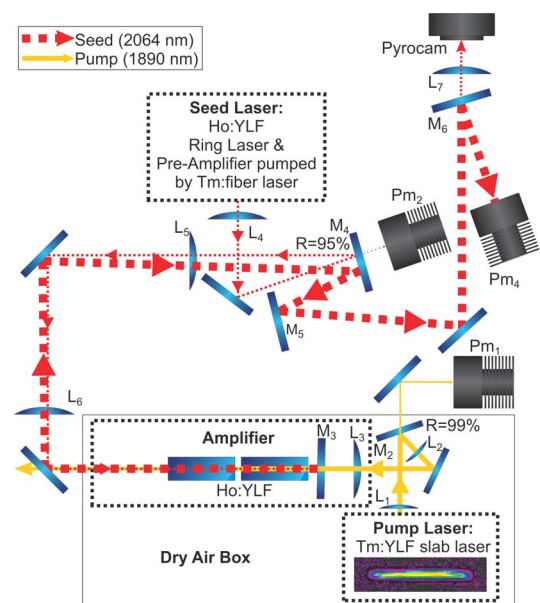


Fig. 1. (Color online) Experimental setup of the double-pass Ho:YLF amplifier.

normal incidence, HR at 2  $\mu\text{m}$ , high transmission (HT) at 1890 nm mirror ( $M_3$ ), which reflected it back for a second pass at a slight horizontal angle to the incident beam direction. The vertical second moment beam radii of the seed beam in the crystals were 0.38 mm on the first crystal surface it encountered and 0.34 mm on the crystal surface closest to  $M_3$ , with similar beam sizes on the return path. In the horizontal plane, a single cylindrical lens  $L_6$  ( $f_x = 2133$  mm) was used to collimate the seed beam to a radius of 3.3 mm. The second pass of the amplified beam was almost spatially symmetrical to the incident beam and passed through cylindrical lenses  $L_6$  and  $L_5$  before being separated by mirror  $M_5$  ( $0^\circ$  HR at 2  $\mu\text{m}$ ) from the seed laser beam. The seed polarization was kept vertical (perpendicular to the crystalline  $c$ -axis) so that it was amplified on the sigma-polarization of the Ho:YLF slabs, which has intrinsic weak thermal lensing [9], at the cost of lower gain due to its lower emission cross section compared to the pi-polarization. Optical feedback into the master ring oscillator/amplifier was prevented by inserting an optical isolator (IO-4-2050-HP from OFR) after the ring oscillator. This reduced the available seed energy incident on the amplifier gain crystals to  $\sim 50$  mJ at 50 Hz.

Various HRs and a partial reflector at 2  $\mu\text{m}$  ( $M_6$ ) reflected the amplified beam onto power meter Pm<sub>4</sub> (LM-45 HTD from Coherent), which measured the average amplified power. The beam contained a continuous wave component which originated from the injection seeding of the Ho:YLF ring laser which was also amplified. This component had a maximum value of 340 mW and was characterized at various 1890 nm pump powers. These were then deducted from the total measured average powers of the amplified pulses.

The amplifier was first optimized at 350 Hz, where the risk of optical damage was the lowest, and the pulse repetition frequency (PRF) was then gradually decreased to 40 Hz. The output results are given in Fig. 2.

The limit where the average power does not increase with PRF was found to be at PRFs above  $\sim 300$  Hz and was  $\sim 43$  W. For lower PRFs, the average output power decreased to  $\sim 12$  W at 40 Hz. The pulse energy increased from 122 mJ at 350 Hz to above 300 mJ at PRFs below 50 Hz, without optical damage. The amplifier was then optimized at low PRFs with respect to seed and pump

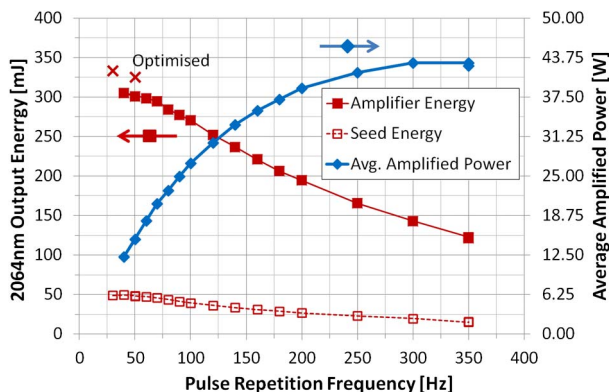


Fig. 2. (Color online) Seed and amplified 2064 nm output energy (left axis) and the average power of the amplified pulses (right axis) as functions of PRF.

alignment. At a minimum PRF of 30 Hz, maximum pulse energy of 333 mJ was obtained. At the required PRF of 50 Hz, 325 mJ was measured (at which subsequent measurements were performed).

The optimized amplifier was subsequently characterized with respect to 1890 nm Tm:YLF pump power and the results are given in Fig. 3. It was estimated that up to 96% of the 1890 nm power was absorbed, dropping to 83% at maximum pump power. This indicated that the total effect of the Ho:YLF pump saturation was minimal due to the long combined length of the slabs. The output energy increased linearly from low levels and slightly rolled over to the maximum output energy of 325 mJ. The slight roll over was attributed to a small increase in beam diameter of the 1890 nm pump beam with power, which was caused by strong negative thermal lensing in the Tm:YLF slab crystal.

From the gain curve (amplified energy/seed energy), it can be seen that the crystals only reached transparency (gain = 1) at  $\sim 41$  W of pump power. At full pump power, the gain increased to  $\sim 5.7$ .

The amplifier performance as a function of the seed energy at full pump power is shown in Fig. 4. The seed energy was varied by placing different partial reflectors into the incident seed beam. The gain at low seed energies was  $\sim 40$ .

The amplified beam transmitted through  $M_6$  was focused by a  $f = 827$  mm lens combination  $L_7$  ( $f = 522 + f = -1415$  mm) to create a waist which was then used to spatially characterize the output using a pyroelectric camera (PYIII-CA from Spiricon). In Fig. 5, the horizontal and vertical second moment beam radii (ISO 11146) are plotted as a functions of the distance from the  $f = 827$  mm lens combination. The beam quality factors in the two transverse directions were determined by fitting the beam radii to the Gaussian beam propagation equation.

The astigmatism was due to the fact that the amplified beam was not shaped with  $L_4$  to be circular symmetric, as well as the astigmatic thermal lens associated with the Ho:YLF amplifier crystals [9]. Figure 6(a) shows the amplified beam intensity profile at maximum output energy. It can be seen that there was a slight degradation in horizontal beam quality. This was also reflected in an increased horizontal beam quality factor ( $M_x^2$ ) of 1.5 and

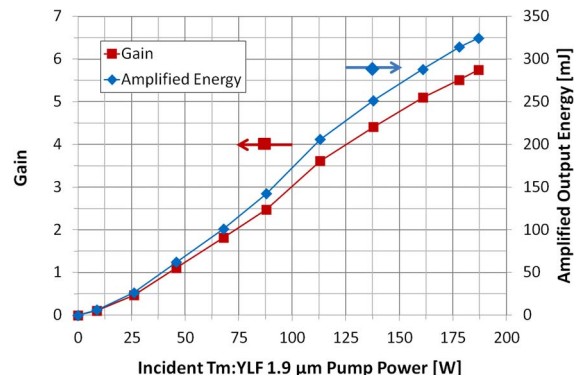


Fig. 3. (Color online) Amplified output energy (right axis) and gain (left axis) as functions of incident 1890 nm Tm:YLF pump power.

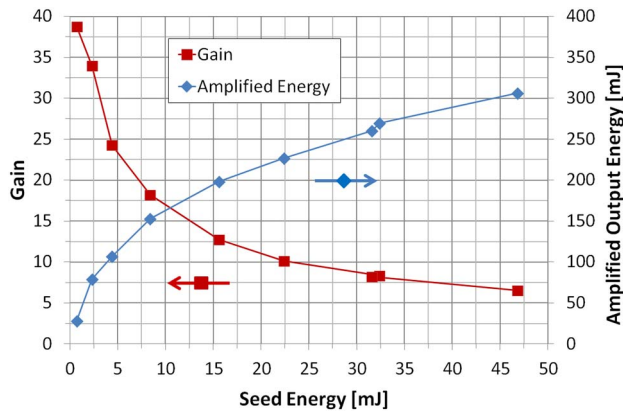


Fig. 4. (Color online) Amplified output energy (right axis) and gain (left axis) as functions of seed energy at a PRF of 50 Hz.

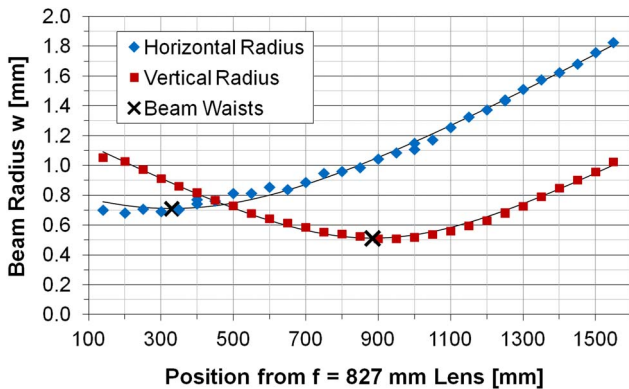


Fig. 5. (Color online) Horizontal and vertical second moment beam radii as functions of distance from an  $f = 827$  mm lens combination at maximum output at 50 Hz. The lines are fits of the beam propagation equation to the measured data and the crosses are the fitted beam waists.

was possibly due to the variation in the horizontal intensity profile of the pump beam, which had a large  $M^2$  value in this direction. In the vertical direction, the beam stayed diffraction limited and had a  $M_y^2$  of 1.01.

It was also verified that the output was single frequency by only observing significant mode-beating when the ring laser was unlocked [10]. The amplified pulse length at full pump power was measured to be  $\sim 350$  ns. This can be seen from the amplified pulse shape that is given juxtaposed with that of the seed in Fig. 6(b). The pulse to pulse energy variation was measured to be less than 5%. The amplified beam was subsequently used to pump an HBr gas laser/amplifier system [11]. The 2064 nm amplified beam was 50% absorbed over an HBr cell with a length of 510 mm (at a pressure of 40 Torr). This implied that its linewidth was narrower than the 400 MHz linewidth of HBr [12].

The output energy can still be significantly scaled. The maximum fluence in the system was calculated to be  $10.9 \text{ J/cm}^2$ , which was still below the optical damage threshold of good quality coatings ( $20\text{--}45 \text{ J/cm}^2$ ) [2,13]. The same architecture can therefore be used to scale the energy at least 3 times higher by simply adding more amplifier modules. However, from calculations [6] we

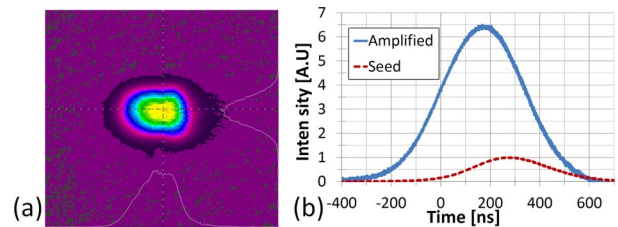


Fig. 6. (Color online) Amplified beam profile in the far field (a) and (b) the seed and amplified pulses at maximum output and a PRF of 50 Hz.

believe that slight modifications to the system in its current form can also lead to improvement. Higher gain is expected if the 28 W of unabsorbed 1890 nm pump power is reflected back into the amplifier crystals. Amplification on the stronger gain, pi-polarization would also be possible if thicker slab crystals were to be used. It was not possible to implement it in this setup because of clipping of the amplified beam due to the relatively strong thermal lensing associated with the pi-polarization of YLF [9].

In conclusion, we have demonstrated a 2064 nm, single-frequency, Ho:YLF slab amplifier, emitting a good quality beam with energies up to 333 mJ. The work shows that Ho:YLF amplifiers, pumped with Tm:YLF slabs, provide an effective way to obtain high energies at 2  $\mu\text{m}$ , which could be scaled even higher using the same architecture.

## References

1. K. Scholle, S. Lamrini, P. Koopmann, and P. Fuhrberg, in *Frontiers in Guided Wave Optics and Optoelectronics*, B. Pal, ed. (InTech, 2010).
2. M. Eichhorn, *Appl. Phys. B* **93**, 269 (2008).
3. B. M. Walsh, N. P. Barnes, and B. Di Bartolo, *J. Appl. Phys.* **83**, 2772 (1998).
4. A. Dergachev, D. Armstrong, A. Smith, T. Drake, and M. Dubois, *Proc. SPIE* **6875**, 687507 (2008).
5. H. J. Strauss, W. Koen, C. Bollig, M. J. D. Esser, C. Jacobs, O. J. P. Collett, and D. R. Preussler, *Opt. Express* **19**, 13974 (2011).
6. O. J. P. Collett, C. Bollig, and M. J. D. Esser, in *CLEO EUROPE and EQEC Conference Digest*, OSA Technical Digest (CD) (Optical Society of America, 2011), paper CA\_P24.
7. C. Bollig, M. J. D. Esser, C. Jacobs, W. Koen, D. Preussler, K. Nyangaza, and M. Schellhorn, in *Mid-Infrared Coherent Sources* (European Physical Society, 2009), invited talk Mo3.
8. L. R. Botha, C. Bollig, M. J. Esser, R. N. Campbell, C. Jacobs, and D. R. Preussler, *Opt. Express* **17**, 20615 (2009).
9. V. V. Zelenogorskii and E. A. Khazanov, *Quantum Electron.* **40**, 40 (2010).
10. A. Dergachev, *Opt. Express* **19**, 6797 (2011).
11. W. Koen, C. Jacobs, C. Bollig, H. J. Strauss, L. Botha, and M. J. D. Esser, *Proc. SPIE* **8543**, 85430E (2012).
12. J. Nicholson, D. Neumann, and W. Rudolph, *Air Force Research Laboratory report AFRL-DE 2001-1015* (Air Force Research Laboratory, 2001).
13. M. Schellhorn and M. Eichhorn, *Appl. Phys. B* **109**, 351 (2012).